ELSEVIER

Journal of Biomechanics 39 (2006) 1726–1734

JOURNAL OF BIOMECHANICS

www.elsevier.com/locate/jbiomech
www.JBiomech.com

Optimal control simulations reveal mechanisms by which arm movement improves standing long jump performance ☆

Blake M. Ashby[a,*], Scott L. Delp[b,c,**]

[a]Department of Mechanical Engineering, The University of Texas at Austin, Austin, TX, USA
[b]Department of Mechanical Engineering, Stanford University, Stanford, CA, USA
[c]Department of Bioengineering, Stanford University, Stanford, CA, USA

Accepted 18 April 2005

Abstract

Optimal control simulations of the standing long jump were developed to gain insight into the mechanisms of enhanced performance due to arm motion. The activations that maximize standing long jump distance of a joint torque actuated model were determined for jumps with free and restricted arm movement. The simulated jump distance was 40 cm greater when arm movement was free (2.00 m) than when it was restricted (1.60 m). The majority of the performance improvement in the free arm jump was due to the 15% increase (3.30 vs. 2.86 m/s) in the take-off velocity of the center of gravity. Some of the performance improvement in the free arm jump was attributable to the ability of the jumper to swing the arms backwards during the flight phase to alleviate excessive forward rotation and position the body segments properly for landing. In restricted arm jumps, the excessive forward rotation was avoided by "holding back" during the propulsive phase and reducing the activation levels of the ankle, knee, and hip joint torque actuators. In addition, swinging the arm segments allowed the lower body joint torque actuators to perform 26 J more work in the free arm jump. However, the most significant contribution to developing greater take-off velocity came from the additional 80 J work done by the shoulder actuator in the jump with free arm movement.

Keywords: Jumping; Whole body coordination; Biomechanical simulation; Optimal control; Arms

1. Introduction

Successful execution of the standing long jump requires the coordination of both upper and lower body segments. In an experimental study of the standing long jump (Ashby and Heegaard, 2002), subjects jumped over 36 cm farther when arm motion was allowed. Greater velocity of the center of gravity (CG) accounted for 24 cm of this improvement. Several explanations have been proposed, but the exact mechanisms for how greater take-off velocity is generated with arm movement have not been established. The purpose of this study was to evaluate three theories for the increased take-off velocity in the standing long jump when arm motion is allowed.

The "hold back" theory suggests that without the ability to swing the arms to remedy excessive forward rotation that would prevent proper landing, the jumper must "hold back" or limit activation of the lower-limb extensors during the propulsive phase. The "joint torque augmentation" theory (Lees et al., 2004) suggests that arm swing generates a downward force at the shoulder on the rest of the body during the propulsion phase,

☆This is James Hay Memorial Award Paper.

*Corresponding author. Tel.: +1 512 471 5718; fax: +1 512 471 8727.

**Corresponding author. James H. Clark Center, Room S-321 Stanford University, MailCode: 5450 318 Campus Drive, Stanford, CA 94305-5450, USA. Tel.: 650 723 1230; fax: 650 725 1587.

E-mail addresses: blake.ashby@stanfordalumni.org, bmashby@mail.utexas.edu (B.M. Ashby), delp@stanford.edu (S.L. Delp).

0021-9290/$ - see front matter © 2005 Elsevier Ltd. All rights reserved.
doi:10.1016/j.jbiomech.2005.04.017

which slows the shortening velocities of the lower body joint extensors and allows for greater muscle torque production (Feltner et al., 1999; Harman et al., 1990). However, as was pointed out by Lees et al. (2004) in their analysis of vertical jumps, the combined effect of greater joint torques with lower angular velocities does not necessarily result in greater power or work generation. The "impart energy" theory is that the muscles crossing the shoulder and elbow joints do work and impart energy that is transferred to the rest of the body (Lees et al., 2004). This added energy of the system may serve to increase the horizontal and vertical displacement and augment the velocity of the CG at take-off.

Optimal control simulations that include a mathematical representation of the objective of a task can provide insight into motor coordination principles (Zajac, 1993). The objective of the standing long jump is clear: maximize the horizontal displacement of the foot without falling upon landing. In the present study, optimal control simulations were developed to find the joint torque activations that maximize performance for jumps with free and restricted arm movement. The results of these simulations were used to evaluate the three theories for the increase in the take-off velocity of the CG in jumps with free arm movement. To address the "hold back" theory, the optimal activations were examined to see if they were lower during the propulsive phase in restricted arm jumps to enable proper positioning of the body segments at landing. The "joint torque augmentation" theory was tested by analyzing the resulting lower body joint torques—and the work done by those torques—to see if they were greater in jumps with free arm movement due to slower extension velocities of the lower body joints. To address the "impart energy" theory, a work/energy analysis was performed to quantify the effect of any additional energy imparted at the shoulder joint in jumps with free arm movement.

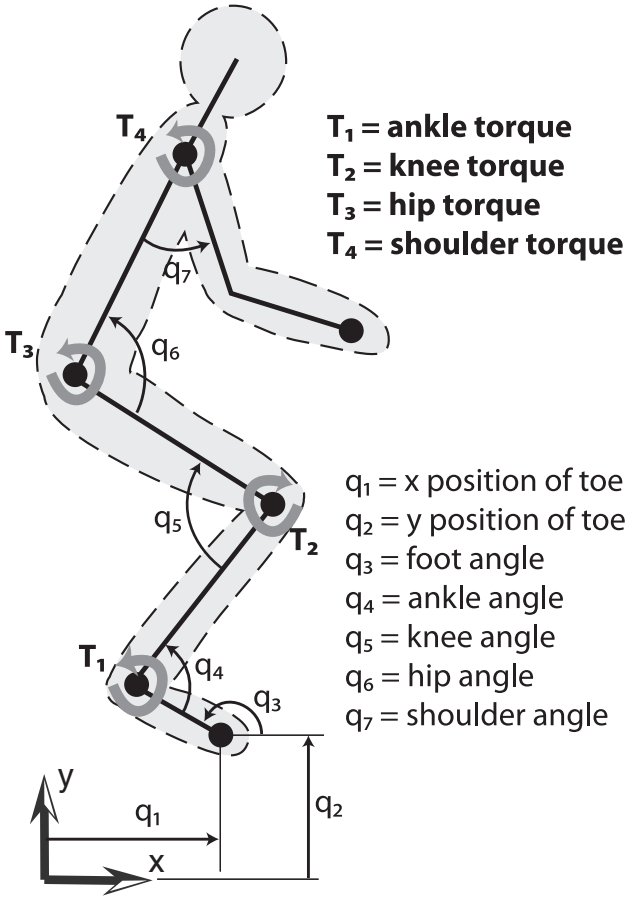

Fig. 1. Two-dimensional, five-segment, seven degree-of-freedom link model actuated by four joint torques used for optimal control simulations.

2. Methods

2.1. Model

The standing long jump was simulated with a two-dimensional, five-segment (foot, shank, thigh, head-neck-trunk, arm), seven degree-of-freedom link model (Fig. 1). The arm segment consisted of upper arm and fore arm segments fused at a fixed elbow joint angle. For restricted arm jumps, the shoulder angle was also fixed throughout the jump. The segmental moments of inertia, lengths, masses, and mass center locations along with the elbow and shoulder joint angles were determined by averaging the respective values from experimental standing long jump studies (Ashby and Heegaard, 2002).

The ankle, knee, hip, and shoulder were actuated by joint torques. The magnitude of each torque depended on the activation (a), the joint angle (q), and the joint angular velocity ($\dot{q}$) according to:

$$T(a, q, \dot{q}) = aT_{\max}(q)T_{\text{vel}}(\dot{q}), \quad (1)$$

where $T_{\max}$ represented the maximum isometric torque that can be generated as a function of the joint angle and T_{vel} was a scaling factor representing the dependence of the torque on the angular velocity of the joint.

The activation (a) of each joint torque could take any value between -1.0 and 1.0. A positive value for a activated the hip and knee extensors, ankle plantar flexors, and shoulder flexors. A negative value for a activated the hip and knee flexors, ankle dorsiflexors, and shoulder extensors. The shapes of the $T_{\max}$ curves were obtained by fitting experimental measurements (doubled to represent both left and right joints) of the maximum isometric joint torques at the ankle (Marsh et al., 1981; Sale et al., 1982), knee (Murray et al., 1977; Scudder, 1980; van Eijden et al., 1987), hip (Inman et al., 1981; Nemeth et al., 1983), and shoulder (Garner and

Pandy, 2001). The joint angular velocity scaling factor (T_{vel}) used when the activation was positive (a similar relationship was used when the activation was negative) was expressed by:

$$T_{vel} = \begin{cases} 0 & \dot{q} > \dot{q}_{max} \\ 1 - \dfrac{1}{\arctan(1.5)} \arctan\left(\dfrac{1.5\dot{q}}{\dot{q}_{max}}\right) & -\dfrac{1}{1.5}\dot{q}_{max} \tan(0.5 \arctan(1.5)) \leqslant \dot{q} \leqslant \dot{q}_{max} \\ 1.5 & \dot{q} > -\dfrac{1}{1.5}\dot{q}_{max} \tan(0.5 \arctan(1.5)). \end{cases} \quad (2)$$

Ligaments at the ankle, knee, hip, and shoulder were modeled by exponential springs (Anderson and Pandy, 1999) to prevent hyperextension or hyperflexion at the extremes of joint motion. The passive ligament torques (T_{lig}) were expressed as a function of joint angle (q) according to:

$$T_{lig} = -100e^{50(q-q_{max}-0.05)} + 100e^{-50(q-q_{min}+0.05)}, \quad (3)$$

where q_{min} and q_{max} represented the minimum and maximum values for the joint angles (70° and 145° for the ankle, 40° and 180° for the knee, 60° and 190° for the hip, and −45° and 180° for the shoulder).

2.2. Optimization

The optimal activations to generate maximum length jumps were found using a simulated annealing algorithm (Corana et al., 1987; Goffe et al., 1994). The activations for the joint torques were each discretized into nodes at every 0.05 s and each node was varied independently during the simulated annealing optimization procedure. The values for the activations in between nodes were determined by linear interpolation.

The equations of motion governing the jumping models were formulated using analytical Lagrangian dynamics techniques for multibody systems. The vertical and horizontal ground contact at the toe was modeled using an augmented Lagrangian formulation that satisfied the inequality constraints at the ground exactly (Ashby, 2004). At each step of the optimization, the equations of motion were integrated from an initially crouched configuration. The initial joint angles and joint angular velocities were consistent with experimental standing long jump studies (Ashby and Heegaard, 2002).

The optimal control problem was to find the values for the joint torque activations ($\boldsymbol{a}$) that minimized a scalar cost function (J) subject to equality constraints that satisfied the equations of motion and inequality constraints that bounded the activations ($-1.0 \leqslant \boldsymbol{a} \leqslant 1.0$). The cost function was represented mathematically by:

$$J = \phi(\boldsymbol{q}, \dot{\boldsymbol{q}})|_{landing} + \int_{t_0}^{t_f} L(\boldsymbol{q}, \boldsymbol{a}, t)\, dt, \quad (4)$$

where ϕ represented jump performance and L included a penalty for activations that did not improve jump distance and a penalty for passive ligament torques throughout the movement.

To test whether "hold back" was necessary to position the body segments properly for landing, the activations that maximized performance were determined for two different cases. The objective for Case 1 was to maximize the horizontal position of the body's CG at landing ($r_x|_{landing}$) without consideration for the landing configuration of the segments. The objective for Case 2 was to maximize the horizontal position of the toe (q_1) at landing while maintaining an acceptable landing configuration.

For Case 1, jump performance was measured by:

$$\phi = r_x|_{landing}. \quad (5)$$

Neglecting air friction, given the position and velocity of the CG at any point in the flight path, and using the equations for projectile motion, $r_x|_{landing}$ was determined uniquely according to:

$$r_x|_{landing} = r_x + \frac{v \cos\theta}{g} \times \left(v \sin\theta + \sqrt{v^2 \sin^2\theta + 2g(r_y - r_y|_{landing})}\right), \quad (6)$$

where r_x is the horizontal position of the CG, r_y is the vertical position of the CG, v is the magnitude of the velocity of the CG, θ is the orientation of the velocity of the CG with respect to the horizontal, g is the gravitational constant, and $r_y|_{landing}$ is the vertical position of the CG at landing.

For Case 2, jump performance was measured by:

$$\phi = -q_1 + K_{CG}, \quad (7)$$

where q_1 was the horizontal position of the toe and K_{CG} was a term that penalized solutions where the CG was too low at landing or where the toe was too far ahead of the CG at landing. To be consistent with experimental jumps (Ashby and Heegaard, 2002), the maximum

distance between the toe and CG at landing was allowed to be 2 cm greater for jumps with free arm movement.

2.3. Work/energy analysis

An energy analysis was performed at the beginning of the movement and also at take-off for Case 2 (constrained landing) simulations. At these two points in time, the total energy, kinetic energy, and potential energy were calculated for the entire system, the body (all segments except the arms), and the arms alone. The work performed for Case 2 simulations between the start time and take-off was calculated for each of the joint actuators by integrating the power ($P = T\dot{q}$) over this period. The work done by the joint actuators was also calculated for Case 1 (unconstrained landing) simulations to determine the effects of arm movement on enhancing performance independent of the effects introduced by the landing constraints.

3. Results

3.1. Jump performance

When the landing configuration of the body was constrained (Case 2), the simulation jumped almost 40 cm farther with free arm movement (2.00 m) than without (1.60 m) (Fig. 2). According to Eq. (6), the 3–4 cm increases in the horizontal (r_x) and vertical (r_y) CG positions at take-off with free arm movement (Table 1) added about 8 cm to r_x at landing. The remaining improvement with arm motion was due to the greater CG take-off velocity for the free arm jump (3.30 m/s) than for the restricted arm jump (2.86 m/s) (Animations 1–4).

3.2. Hold back

With free use of the arms, the horizontal position of the CG (r_x) at landing was 1.68 m when there were no

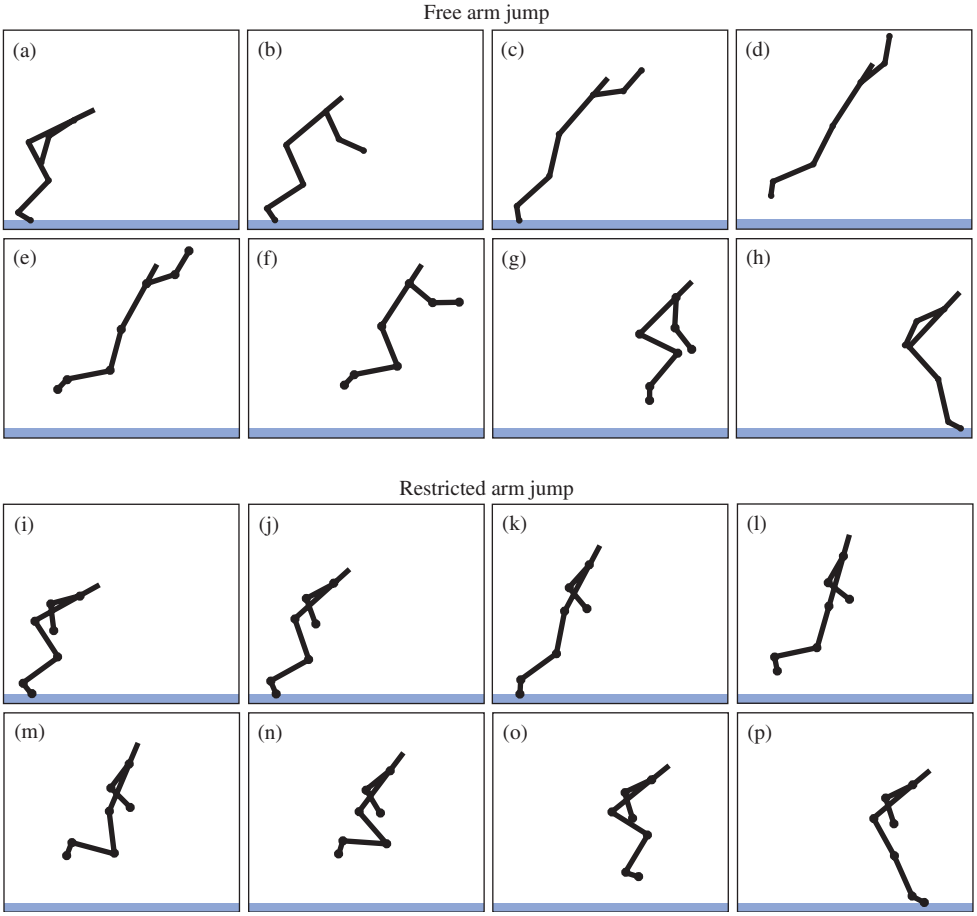

Fig. 2. Body configuration for constrained landing jumps (Case 2) with free (top) and restricted (bottom) arm movement at eight instants in time. For the free arm jump, during the ground contact phase (a–c) the arms were swung forwards until take-off (c). During the flight phase (d–h), the arms were swung backwards to properly position the body for landing (h). In the restricted arm jump, the horizontal and vertical displacement of the mass center at take-off (k) was less because the model could not extend the arms ahead and above the body. The horizontal displacement of the toe at landing (h and p) was 40 cm less in the restricted arm jump. Also see animations of the jumps in the supplementary website material.

Table 1
Kinematic parameters at take-off and landing for free and restricted arm jumps

	Free arms		Restricted arms	
	Case 1	Case 2	Case 1	Case 2
q_1 (horizontal position of toe) at landing (m)	n/a	2.00	n/a	1.60
r_x (horizontal position of CG) at landing (m)	1.68	1.66	1.37	1.29
r_x (horizontal position of CG) at take-off (m)	0.53	0.52	0.49	0.49
r_y (vertical position of CG) at take-off (m)	0.90	0.90	0.87	0.86
v (CG velocity magnitude) at take-off (m/s)	3.32	3.30	2.93	2.86
θ (CG velocity angle w/r to horizontal) at take-off (°)	36.0	36.1	37.1	34.1

Case 1: maximize horizontal position of the CG (r_x) at landing with no landing constraints.
Case 2: maximize toe position (q_1) at landing with landing constraints.

requirements on the landing configuration (Case 1). When an acceptable landing configuration was required (Case 2), r_x at landing was decreased by only just over 1 cm. When arm motion was restricted, r_x at landing was 1.37 m for Case 1 and 8 cm less (1.29 m) for Case 2. The landing requirements reduced jump performance in restricted arm jumps more than in free arm jumps, indicating that the simulated jumper had to "hold back" during the propulsive phase in jumps with restricted arm movement to position the body segments properly for landing.

The lower body activations for jumps with free arm movement were virtually indistinguishable for the constrained (Case 2) and unconstrained (Case 1) landing cases (left column of Fig. 3). Little modification in the control strategy was necessary when the constraint on the landing configuration was introduced, because the extra control provided by the arms allowed the model to successfully manipulate the body segments for landing. However, in jumps with restricted arm motion, the lower body activations were different when the landing constraint was imposed (right column of Fig. 3). For restricted arm jumps, the ankle activation was lower from −0.15 s to −0.075 s, the knee activation was lower until −0.075 s, and the hip activation was lower from −0.025 s until take-off in the constrained landing jump (Case 2) than in the unconstrained landing jump (Case 1). The solutions found by the optimization routine show that when arm movement was not allowed, the simulation had to "hold back" and limit activation of the lower body joints to maximize jump distance while landing properly.

3.3. Joint torque augmentation

The torque generated by the hip joint actuator was greater throughout the ground contact phase for the constrained landing jump (Case 2) with free arm movement (top plot in Fig. 4). Until −0.12 s, the hip torque was greater when arm motion was allowed because the activation was higher (middle plot in Fig. 4). After that time, the difference in joint torque was caused by the difference in hip extension velocities (bottom plot in Fig. 4). In the jump with free arm movement, the shoulder flexion torque and greater downward reaction force at the shoulder slowed the backward rotation of the trunk, which slowed the extension velocity of the hip.

Until about −0.10 s, the knee extension torque was greater (top plot in Fig. 5) for the constrained landing jump (Case 2) with restricted arm movement because the activation was higher (middle plot in Fig. 5). After this time, the knee joint torque levels were similar until take-off.

The torque generated at the ankle was greater throughout the ground contact phase for the constrained landing jump (Case 2) with free arm movement (top plot in Fig. 6). Greater activation for most of this period when arm motion was allowed (middle plot in Fig. 6) was the primary cause of the greater torque. However, for the period between −0.075 s and −0.025 s when the ankle actuators were fully activated for both types of jumps, the torque was greater for the jump with free arm movement because the extension velocity of the ankle was lower (bottom plot in Fig. 6). Through complex interactions among the rotating segments, swinging the arms slowed the rate of extension of the ankle over this period and allowed for greater torque generation.

Enhanced joint torques do not necessarily lead to enhanced performance. Since the increased joint torques at the hip and ankle were achieved because of lower angular velocities, the resulting joint power and work done (joint power integrated over time) might not have been higher. When the landing configuration was constrained (Case 2), the lower body joints combined to do 26 J more work in jumps with free arm movement (Table 2). In the free arm jump, the ankle and hip actuators both performed more work (25 J and 21 J more, respectively), but the knee actuator performed 19 J less. Some of this increase in work was due to the simulation "holding back" in restricted arm jumps.

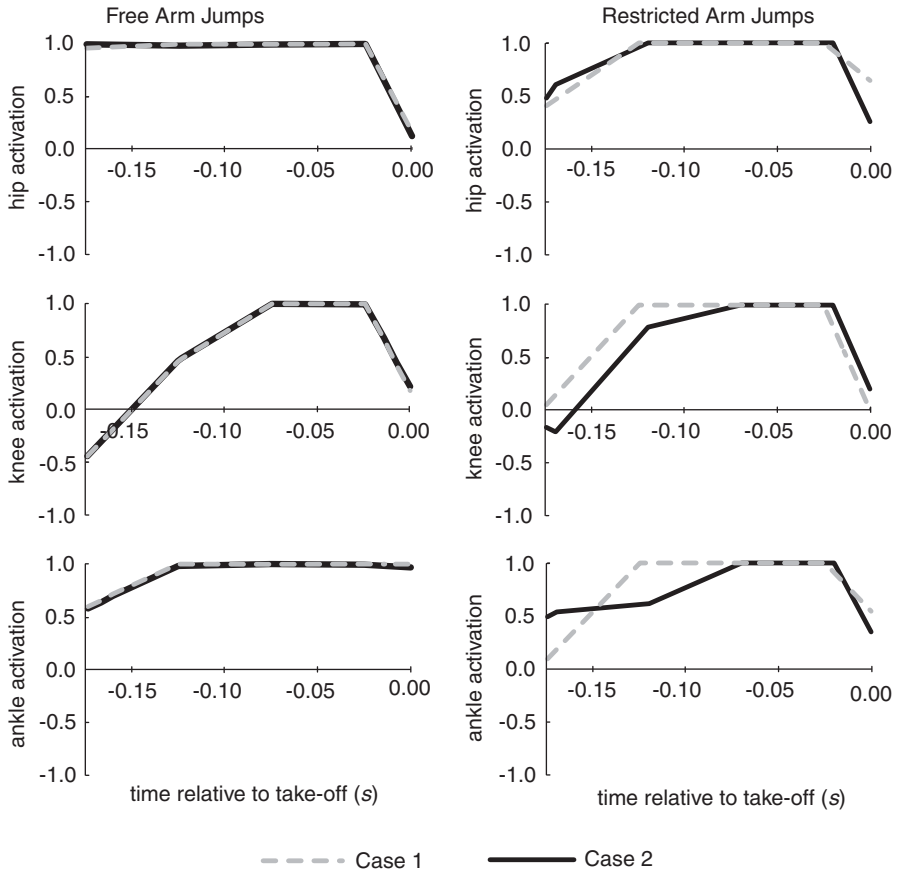

Fig. 3. Activations for lower body joint (ankle, knee, and hip) actuators for jumps with free (left column) and restricted (right column) arm movement for unconstrained (Case 1—gray dashed line) and constrained (Case 2—solid line) landing. For free arm jumps, the activations were almost indistinguishable for the two cases indicating that when arm movement was allowed, the simulations did not have to alter the optimal activations during the ground contact phase to handle the landing constraints. For restricted arm jumps, the activations were noticeably different for the two cases indicating that when arm motion was restricted, the simulations had to make significant changes in the optimal control strategies (i.e., "hold back") to handle the landing constraints.

When the landing constraint was removed (Case 1), the lower body joints still did more work in free arm jumps, but only 13 J more. Thus, the results of these simulations support the theory that arm swing augments the ability of lower body muscles to both generate torque and perform work.

3.4. Impart energy

At the start time for the constrained landing simulations, the model with free arm movement already had 87 J more total energy than the model with restricted arm movement (624 J compared with 537 J). Most of the difference was due to an 80 J difference in the kinetic energy of the swinging arm segments.

At take-off, the total energy of the system increased to 1190 J for the free arm jump and 996 J for the restricted arm jump, a difference of 194 J (Table 3). A small part (27 J) of this difference was due to the difference in potential energy of the two models that was mostly due to the extra height achieved by the arms. Most (167 J) of the difference in total energy was due to the increased kinetic energy in the jump with free arm movement. The kinetic energy of the arms (104 J greater) and the rest of the body segments (63 J greater) were both substantially greater at take-off when arm motion was allowed.

The increase in total energy between the start time and take-off is entirely due to the work done by the joint torque actuators. During this period, 566 J of work was performed in the free arm jump and 460 J of work was performed in the restricted arm jump, a difference of 106 J (Table 2). Most (80 J) of this difference was due to the additional work done at the shoulder joint in the jump with free arm motion.

The "impart energy" theory that the muscles spanning the shoulder do work and impart energy to the system that can be used to increase the CG velocity at take-off is supported by these simulations. The extra energy at take-off in free arm jumps came primarily from two sources: (1) the extra kinetic energy in the swinging arms (80 J) at the start time of the simulation and (2) the extra work done by the shoulder joint torque actuators (80 J).

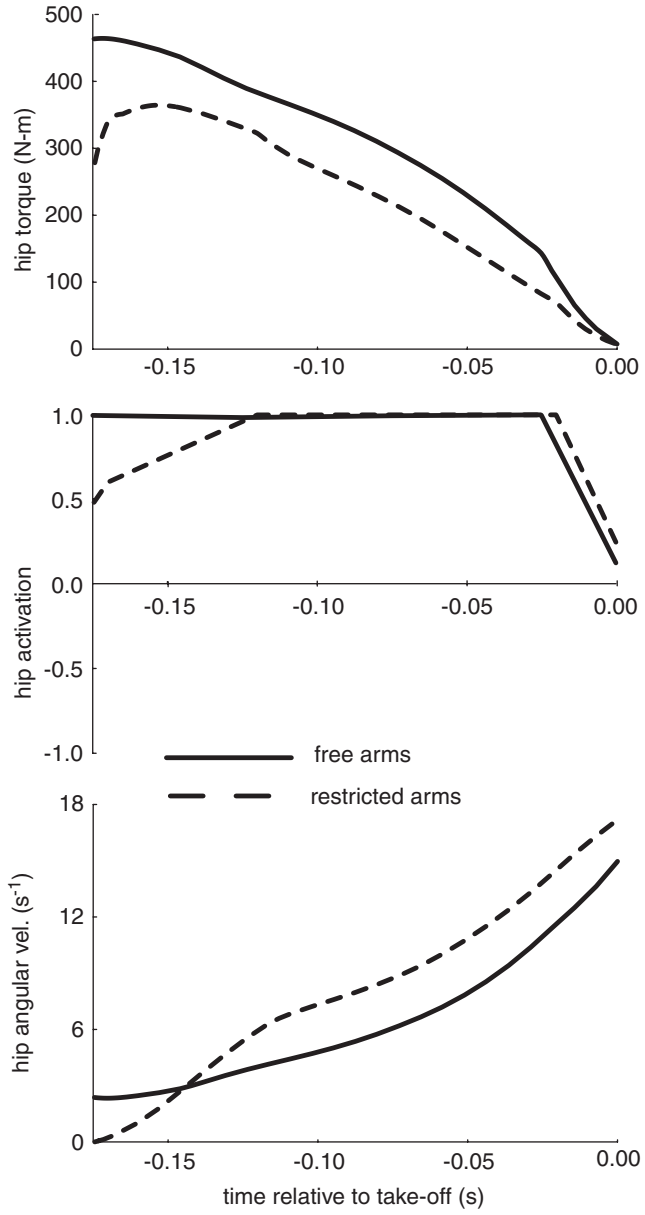

Fig. 4. Hip torque (top), activation (middle), and angular velocity (bottom) for constrained landing jumps (Case 2) with free and restricted arm movement. Until −0.12 s, the torque is higher in the free arm jump because the activation is higher. From −0.12 s until take-off, the torque is higher in the free arm jump because the hip extension velocity is lower.

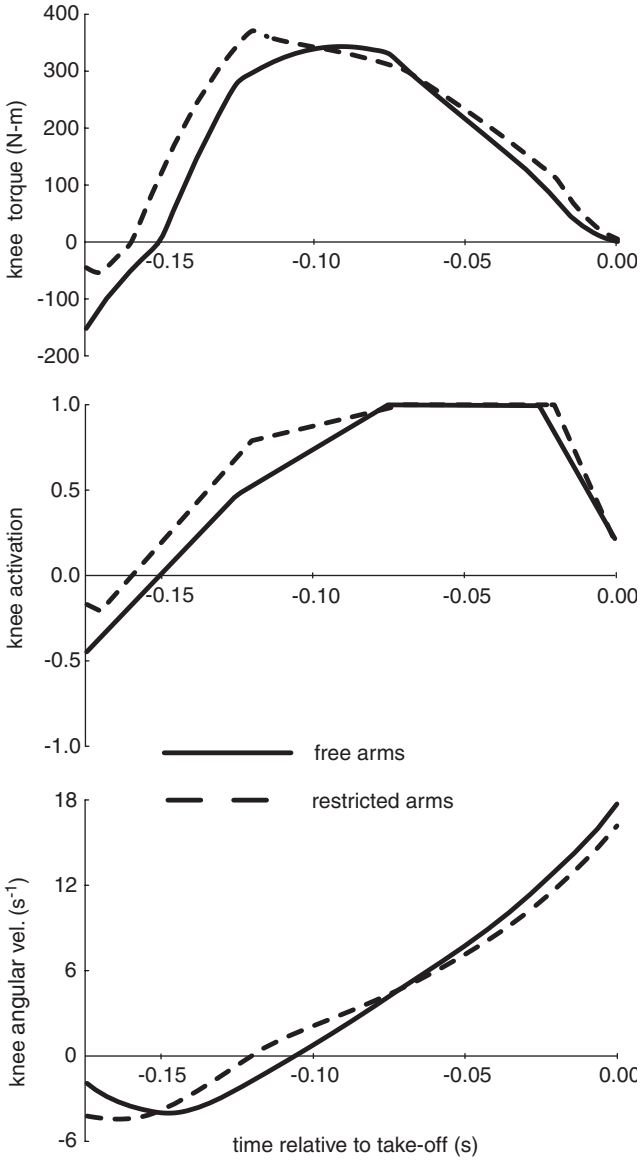

Fig. 5. Knee torque (top), activation (middle), and angular velocity (bottom) for constrained landing jumps (Case 2) with free and restricted arm movement. The knee torque for the restricted arm jump was higher until −0.10 s because the activation was higher. From this point the knee torques were similar until take-off.

4. Discussion

This study showed that arm motion enhances standing long jump performance because of the increased horizontal and vertical positions and velocities of the CG at take-off. The "hold back", "joint torque augmentation", and "impart energy" theories for how the extra take-off velocity of the CG is generated were all tested and found to contribute to performance improvement in the standing long jump. The mechanisms involved in all three of these theories worked together to develop greater take-off velocity. The most significant contribution came from the additional energy imparted to the system by the work done by the shoulder actuator.

"Joint-torque augmentation" due to swinging the arms has also been shown to occur in experimental studies of the standing high jump (Feltner et al., 1999; Lees et al., 2004). However, Lees et al. (2004) rejected the "joint torque augmentation" theory, noting that in free arm jumps during the periods where the joint torques were higher because of lower angular velocities, less power was being generated. While this is true, the

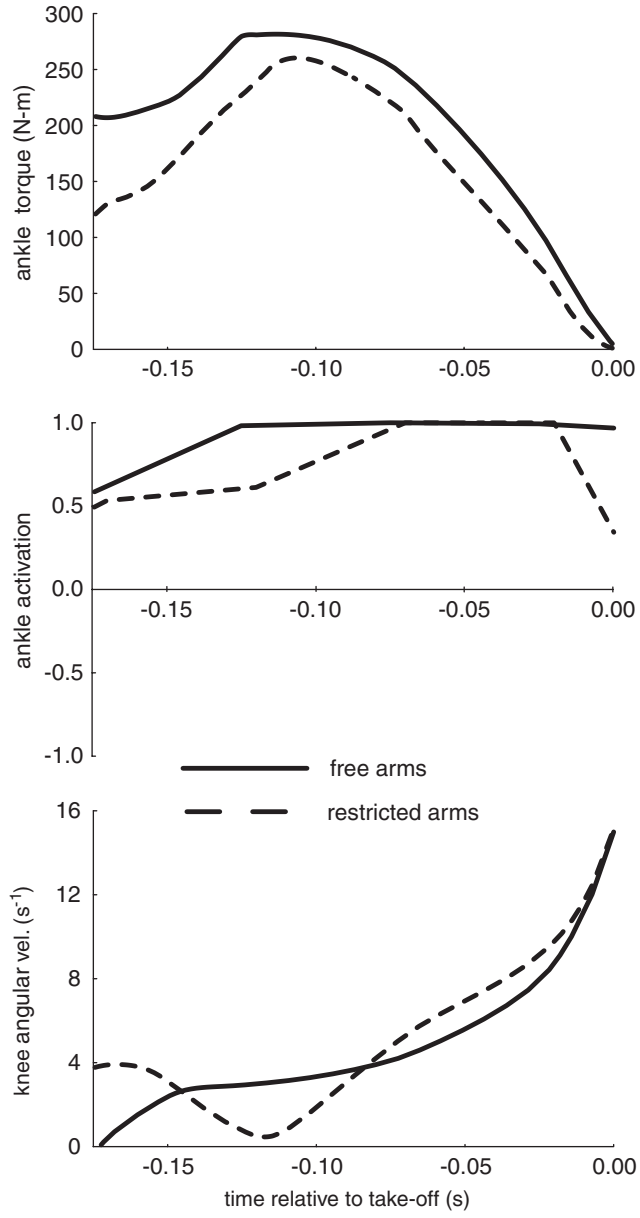

Fig. 6. Ankle torque (top), activation (middle), and angular velocity (bottom) for constrained landing jumps (Case 2) with free and restricted arm movement. Between −0.075 s and −0.025 s the ankle actuators were fully activated for both types of jumps, but the torque was greater for the free arm jump because the ankle angular velocity was lower. The ankle torque was higher in the free arm jump during the remaining periods of the ground contact phase because the activation was higher.

key measure in imparting energy to the system is work, not power (the time derivative of work). They reported that between the low point in the countermovement jump to the apex of the flight phase, the work done at the ankle and knee was basically the same for the two types of jumps, but the work done at the hip was 14% greater in free arm jumps. Thus, in their study, arm swing enhanced the hip extensors' ability to do work.

Table 2
Work done until take-off for constrained landing jumps (Case 2)

	Free arms	Restricted arms	Difference
Total work done (W)	566	460	106
Work done at lower body joints	486	460	26
W_{ankle}	135	110	25
W_{knee}	99	118	−19
W_{hip}	253	232	21
Work done at shoulder ($W_{shoulder}$)	80	0	80

All units are J.

Table 3
Energy breakdown at take-off for constrained landing jumps (Case 2)

	Free arms	Restricted arms	Difference
Total energy	1190	996	194
Potential energy (PE)	637	610	27
PE_{body}	521	516	5
PE_{arms}	116	94	22
Kinetic energy (KE)	553	386	167
KE_{body}	389	326	63
KE_{arms}	164	60	104

All units are J.

Many of the results from these simulations are consistent with the results from the experimental studies (Table 4) (Ashby and Heegaard, 2002). The experimental jump distances (horizontal position of the toe at landing) were 9–12 cm greater. Most of that difference is due to the greater horizontal and vertical positions of the CG at take-off in the experiments. The main reason for this difference is that the simulation did not include a segment for the phalanges (toes). Including an 8–10 cm long toe segment would have allowed the body to extend that much farther at take-off. The CG velocities at take-off for jumps with free and restricted arm movement were both within 3% of the experimental take-off velocities.

As with all simulations, the assumptions and simplifications made in constructing the model limit the types of questions that can be addressed. First, using joint torque actuators instead of musculotendon actuators limits the model's ability to answer questions about the role of individual muscles in jumping. Second, activation dynamics describing the time lag between the neural excitation and the corresponding muscle (or joint torque) activation (Zajac, 1989) was not included in these simulations. Therefore, the optimal control routines solved for the optimal *activations* rather than the optimal *neural controls*. Implicit in this simplification was the assumption that a set of neural controls exist that could produce these activations. Third, the landing

Table 4
Comparison of kinematic results at take-off and landing from optimal control simulations for constrained landing jumps (Case 2) and experimental studies of the standing long jump (Ashby and Heegaard, 2002)

	Free arms		Restricted arms	
	Experiment	Simulation	Experiment	Simulation
q_1 at landing (m)	2.09	2.00	1.72	1.60
r_x at take-off (m)	0.57	0.52	0.49	0.49
r_y at take-off (m)	0.97	0.90	0.95	0.86
v at take-off (m/s)	3.32	3.30	2.95	2.86

phase was not modeled. By modeling impact at landing, the hypothesis that free arm movement allows the jumper to extend the toes farther in front of the CG at landing could be evaluated. Fourth, these simulations assumed that the standing long jump is executed in the sagittal plane. For the most part this is a valid assumption, but experimental studies have shown that some jumpers use out-of-plane movements with their arms during portions of the flight phase (Ashby and Heegaard, 2002). A 3-D simulation could be useful in determining what benefits, if any, this out-of-plane movement provides. Finally, the simulation began in a crouched position, so the optimal activations were determined only for the propulsive phase of the movement. When the simulation began, the jump with free arm movement had already developed 87 J more energy. Solving for the activations in the earlier stages of the movement would provide additional insight into the role of arm motion in enhancing jump performance.

Acknowledgments

Blake M. Ashby has been supported by a William R. and Sara Hart Kimball Stanford Graduate Fellowship and a Veterans Affairs Rehabilitation Research and Development Fellowship. Special thanks is given to Dr. Jean Heegaard for his help with the development of the optimal control simulations.

Appendix A. Animation

The online version of this article contains additional supplementary data. Please visit doi:10.1016/j.jbiomech.2005.04.017.

References

Anderson, F.C., Pandy, M.G., 1999. A dynamic optimization solution for vertical jumping in three dimensions. Computer Methods in Biomechanics and Biomedical Engineering 2, 201–231.

Ashby, B.M., 2004. Coordination of upper and lower limbs in the standing long jump: kinematics, dynamics, and optimal control. Ph.D. Thesis, Stanford University.

Ashby, B.M., Heegaard, J.H., 2002. Role of arm motion in the standing long jump. Journal of Biomechanics 35, 1631–1637.

Corana, A., Marchesi, M., Martini, C., Ridella, S., 1987. Minimizing multimodal functions of continuous variables with the 'simulated annealing' algorithm. ACM Transactions on Mathematical Software 13, 262–280.

Feltner, M.E., Fraschetti, D.J., Crisp, R.J., 1999. Upper extremity augmentation of lower extremity kinetics during countermovement vertical jumps. Journal of Sports Sciences 17, 449–466.

Garner, B.A., Pandy, M.G., 2001. Musculoskeletal model of the upper limb based on the visible human male dataset. Computer Methods in Biomechanics and Biomedical Engineering 4, 93–126.

Goffe, W.L., Ferrier, G.D., Rogers, J., 1994. Global optimization of statistical functions with simulated annealing. Journal of Econometrics 60, 65–99.

Harman, E.A., Rosenstein, M.T., Frykman, P.N., Rosenstein, R.M., 1990. The effects of arms and countermovement to vertical jumping. Medicine and Science in Sports and Exercise 22, 825–833.

Inman, V.T., Ralston, H.J., Todd, F., 1981. Human Walking. Williams & Wilkins, Baltimore.

Lees, A., Vanrenterghem, J., de Clercq, D., 2004. Understanding how an arm swing enhances performance in the vertical jump. Journal of Biomechanics 37, 1929–1940.

Marsh, E., Sale, D., McComas, A.J., Quinlan, J., 1981. Influence of joint position on ankle dorsiflexion in humans. Journal of Applied Physiology 51, 160–167.

Murray, M.P., Baldwin, J.M., Gardner, G.M., Sepic, S.B., Downs, W.J., 1977. Maximum isometric knee flexor and extensor muscle contractions. Physical Therapy 57, 637–643.

Nemeth, G., Ekholm, J., Arborelius, U.P., Harms-Ringdahl, K., Schuldt, K., 1983. Influence of knee flexion on isometric hip extensor strength. Scandinavian Journal Rehabilitation Medicine 15, 97–101.

Sale, D., Quinlan, J., Marsh, E., McComas, A.J., Belanger, A.Y., 1982. Influence of joint position on ankle plantarflexion in humans. Journal Applied Physiology 52, 1636–1642.

Scudder, G.N., 1980. Torque curves produced at the knee during isometric and isokinetic exercises. Archives of Physical Medicine and Rehabilitation 61, 68–72.

van Eijden, T.M.G.J., Weijs, W.A., Kouwenhoven, E., Verberg, J., 1987. Forces acting on the patella during maximal voluntary contraction of the quadriceps femoris muscles at different knee flexion/extension angles. Acta Anatomica 129, 310–314.

Zajac, F.E., 1989. Muscle and tendon: properties, models, scaling, and application to biomechanics and motor control. Critical Reviews in Biomedical Engineering 17, 359–411.

Zajac, F.E., 1993. Muscle coordination of movement: a perspective. Journal of Biomechanics 26, 109–124.